Selectively Micro-Patternable Fibers via In-Fiber Photolithography

ACS central science

http://pubs.acs.org/journal/acscii

Research Article

Selectively Micro-Patternable Fibers via In-Fiber Photolithography

Youngbin Lee, Andres Canales, Gabriel Loke, Mehmet Kanik, Yoel Fink, and Polina Anikeeva*

Cite This: ACS Cent. Sci. 2020, 6, 2319–2325

Read Online

ACCESS | Metrics & More | Article Recommendations | Supporting Information

ABSTRACT: Multimaterial fibers engineered to integrate glasses, metals, semiconductors, and composites found applications in ubiquitous sensing, biomedicine, and robotics. The longitudinal symmetry typical of fibers, however, limits the density of functional interfaces with fiber-based devices. Here, thermal drawing and photolithography are combined to produce a scalable method for deterministically breaking axial symmetry within multimaterial fibers. Our approach harnesses a two-step polymerization in thiol−epoxy and thiol−ene photopolymer networks to create a photoresist compatible with high-throughput thermal drawing in atmospheric conditions. This, in turn, delivers meters of fiber that can be patterned along the length increasing the density of functional points. This approach may advance applications of fiber-based devices in distributed sensors, large area optoelectronic devices, and smart textiles.

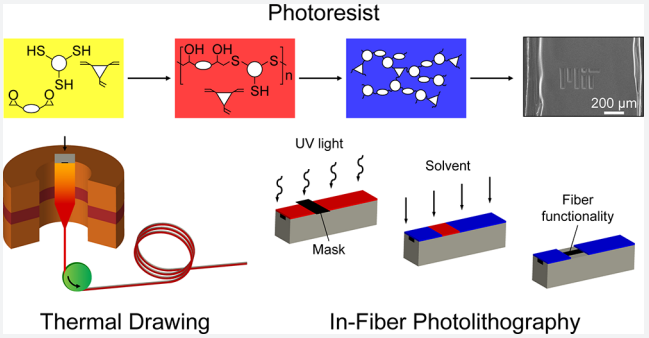

INTRODUCTION

Multimaterial fibers composed of polymers, metals, and semiconductors[1−3] expand the range of applications of fiber technology to sensors,[4−8] electronics,[9−13] biomedicine,[14−18] and smart textiles.[19−24] Multimaterial fabrication affords sophisticated integration of a diversity of functional elements within individual filaments including electrodes,[5−16,20,21,23] diodes,[20] microfluidic channels,[6,14,16] optical waveguides,[7,14,16] and piezoelectric sensors,[11] while preserving benefits intrinsic to fibers including high-throughput production, micro- to nanoscale features, and mechanical flexibility. However, the interfaces of fibers with other systems are largely limited to their tips, which impedes their applications in large area applications. While longitudinal symmetry in fibers can be broken through selective capillary breakup,[12] gaining electrical, optical, or fluidic access to the devices embedded within the fiber cladding commonly relies on the low-throughput ablation methods.[25,26] A method offering access to functional features along the fiber lengths would expand the capabilities and interface density of fiber-based systems.

Here, we combine two high-throughput methods: thermal drawing and in-fiber photolithography, to create meters-long fibers with microscale patterns along the surfaces. Unlike prior research relying on coating of photoresists onto fiber surfaces or tips to enable lithographic patterning,[27−31] our approach develops a high-throughput thermally drawable photoresist based on a thiol−epoxy/thiol−ene network with thermal and photopolymerization properties. Our approach enables deterministic breaking of the conventional longitudinal symmetry in fibers and paves the way toward high-density interfaces with the embedded functional elements within fibers. By producing hundreds of meters of lithographically enhanced fibers, our approach may advance applications of fiber-based devices in large-area electronics, smart textiles, and distributed sensing.

RESULTS AND DISCUSSION

We developed a thermally drawable photoresist to enable photolithographic patterning at arbitrary points along the fiber length. A drawable photoresist should satisfy two materials design criteria. First, it has to be a thermoplastic with a glass transition temperature (T_g) which is in a similar range with process temperatures of other materials constituting functional elements of a multimaterial fiber. This implies that, at temperatures $T > T_g$, a photopolymer could be aligned and stretched along the drawing direction while avoiding complete cross-linking during fiber fabrication. Second, a photolithographic patterning of a drawn fiber constituent, termed here as "in-fiber photolithography", favors negative photoresists, because the cross-linked structure characteristic of positive photoresists[32] prevents the rheological flow required for thermal drawing. In contrast, the incomplete or non-cross-linked structure of negative photoresists permits their fiber processing.

We found that a thiol−epoxy/thiol−ene photopolymer network can be engineered to satisfy the thermally drawable

Received: September 3, 2020
Published: November 25, 2020

https://dx.doi.org/10.1021/acscentsci.0c01188
ACS Cent. Sci. 2020, 6, 2319−2325

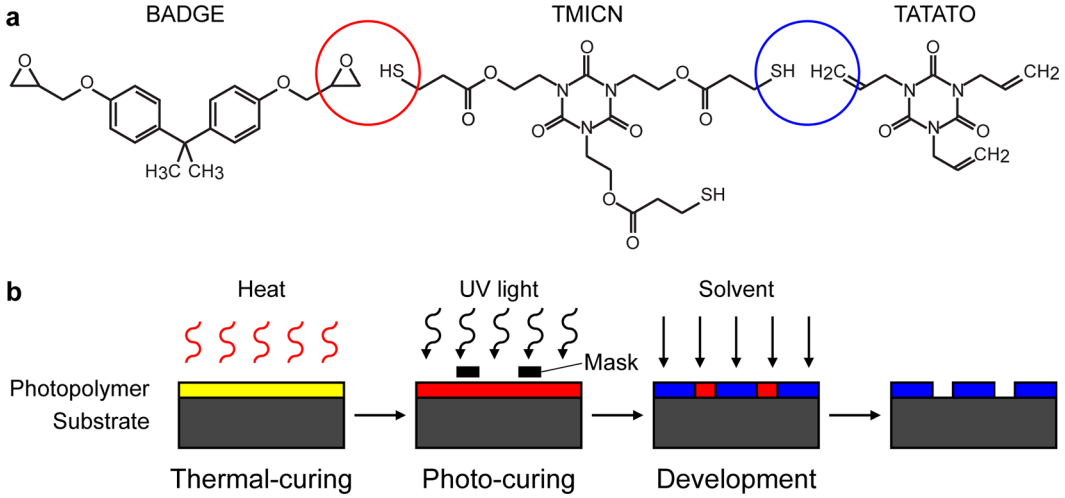

Figure 1. Thiol−epoxy/thiol−ene photopolymer. (a) Components of the photopolymer composite. The red and blue circles represent functional groups reacting during thermal and photocuring, respectively. (b) Schematic of the photolithographic patterning process of the thiol−epoxy/thiol−ene network. The yellow, red, and blue colors denote the noncured, the thermally cured, and the photocured photoresist. Gray color marks the substrate.

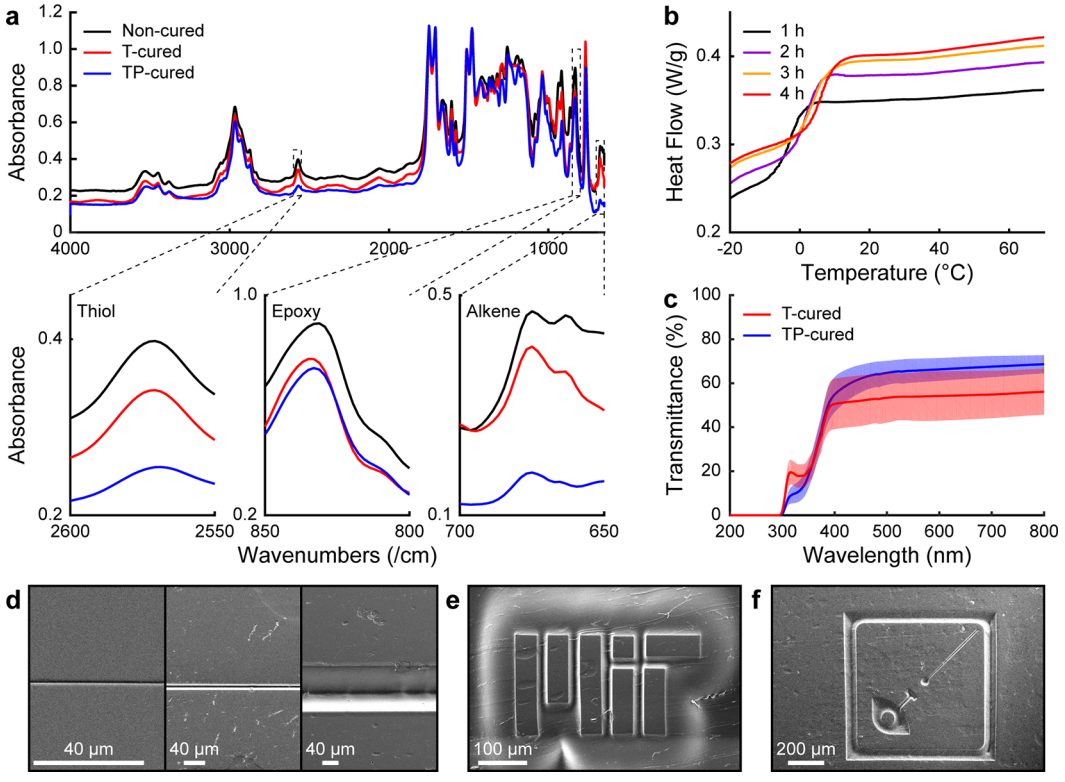

Figure 2. Characterization of thiol−epoxy/thiol−ene photopolymer. (a) Fourier-transform infrared spectroscopy (FTIR) measurements are shown for the photopolymer in the uncured (black), thermally (T) cured (red), and photocured (TP) (blue) state. Peaks in the ranges 2550−2600, 800−850, and 650−700/cm correspond to thiol, epoxy, and alkene functional groups, respectively. (b) Differential scanning calorimetry (DSC) shows the increase in the photopolymer T_g following 1 (black), 2 (purple), 3 (amber), and 4 (red) hours of thermal-cuing, respectively. (c) UV−vis transmittance spectra of the photopolymer prior to (red) and following (blue) photocuring. All samples have been thermally cured. Shaded areas denote standard deviation (n = 5 samples). (d−f) Scanning electron microscope (SEM) images of patterns lithographically defined on the free-standing photopolymer films. (d) Line patterns with 1, 10, and 100 μm thickness. (e,f) Geometric patterns.

photoresist design criteria. Thiol−ene chemistry has been widely used in coatings and traditional lithography due to its low inhibition of oxygen and minimal mechanical deformation during polymerization.[32,33] However, low melting temperatures of the monomer components of the thiol−ene photoresist prior to light exposure make them incompatible with thermal codrawing with high-performance thermoplastics, glasses, and composites comprising functional fibers. To enable thermal drawing of the thiol−ene system alongside other materials, a monomer with epoxy functional group was added to create a thermoplastic with T_g via thiol−epoxy polymerization.[34,35] For our thiol−epoxy/thiol−ene based drawable

https://dx.doi.org/10.1021/acscentsci.0c01188
ACS Cent. Sci. 2020, 6, 2319−2325

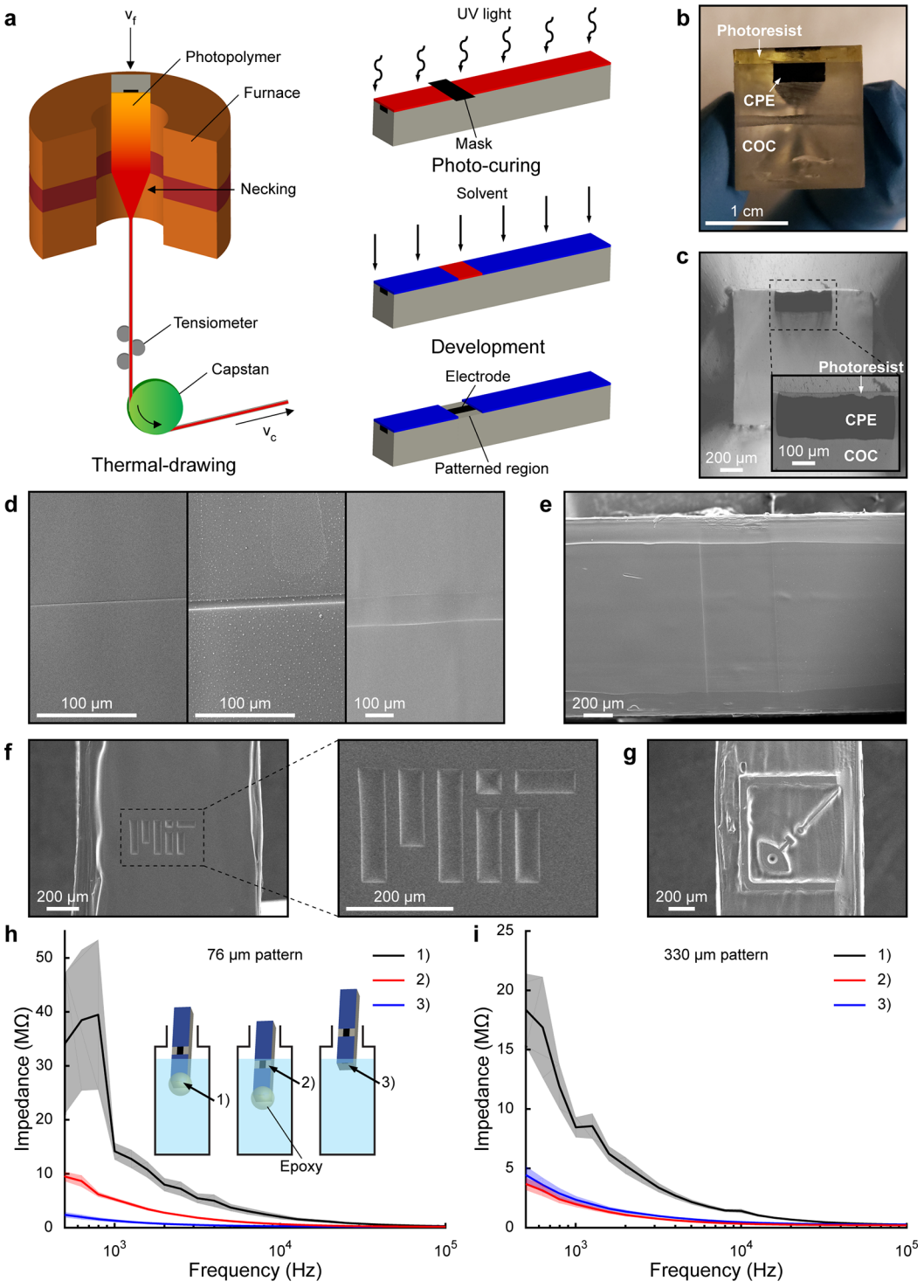

Figure 3. In-fiber photolithography. (a) Schematic depicting thermal drawing and lithographic patterning of the multimaterial fibers. Cyclic olefin copolymer (COC), carbon-loaded polyethylene (CPE), and thiol−epoxy/thiol−ene photopolymer are marked with gray, black, and orange to red gradient colors, respectively. Red and blue colors represent thermally and photocured photopolymer, respectively. (b) Cross-sectional image of the preform prior to thermal drawing. (c) Cross-sectional image of the fiber thermally drawn from the preform in panel (b). An inset presents a higher magnification image of the photopolymer layer coating the CPE conductor. (d−g) SEM images of patterns developed directly on the thermally drawn fibers. (d) Line patterns with 1, 10, and 100 μm thicknesses. (e) Thermally drawn fiber with a line pattern of 500 μm thickness. (f,g) Geometric patterns. (h,i) Impedance spectra of the CPE electrodes within the thermally drawn fibers exposed along the length via (h) 76 μm and (i) 330 μm line patterns. The black, red, and blue curves present the mean impedance of CPE electrode under the conditions shown in the inset. (1) Open circuit measurement of the epoxy-insulated fiber tip in PBS. (2) Measurement of the CPE electrode exposed along the fiber shaft. (3) CPE electrode tip impedance. Shaded areas represent standard error (n = 5 samples).

photoresist, tris[2-(3-mercaptopropionyloxy)ethyl] isocyanurate (TMICN), bisphenol A diglycidyl ether (BADGE), and 1,3,5-triallyl-1,3,5-triazine-2,4,6 (1H,3H,5H)-trione (TATATO) were selected as monomers with thiol, epoxy and alkene

https://dx.doi.org/10.1021/acscentsci.0c01188
ACS Cent. Sci. 2020, 6, 2319−2325

functional groups, respectively (Figure 1a). This thiol−epoxy/thiol−ene system enables independent thermal and photopolymerization based on click chemistry between the thiols and epoxy or alkene functional groups, respectively (Figure S1).[35] During thermal-curing, the alternating thiol trifunctional TMICN and epoxy bifunctional BADGE form a linear or branched thermoplastic polymer compatible with thermal drawing. During photocuring under ultraviolet (UV) light, a thiol−ene reaction between the remaining thiol functional groups of TMICN and alkene trifunctional groups of TATATO results in cross-linking that renders the network insoluble in common solvents such as acetone and tetrahydrofuran (Figure 1b).

The decrease in the number of functional end groups at each polymerization step was observed in the Fourier-transform infrared (FTIR) spectra (Figure 2a). Differential scanning calorimetry (DSC) shows that as the thermal-curing time increases, the T_g of the thiol−epoxy/thiol−ene system increases, which can likely be attributed to the formation of longer polymer chains. This may allow for tailoring of the photoresist thermomechanical properties to those of the other fiber components of interest (Figure 2b). Photopolymerization is further detected as an increase in transmission in the visible spectra due to the decrease in the number of conjugated bonds following thiol−ene reaction (Figure 2c).[36] Together, these analyses indicated that the thiol−epoxy/thiol−ene system forms a thermally polymerized negative photoresist. Consistent with these measurements, we find that the system permits the development of patterns with a resolution of at least 1 μm (Figure 2d−f). This resolution most likely presents an upper bound for achievable feature dimensions, and significant improvements could be attained through employing collimated light sources.

To optimize the photopolymer composition for the thermal drawing and photolithography, we performed photopatterning on films of the thiol−epoxy/thiol−ene networks with different compositions following their thermal curing at the drawing temperature (Supporting Information). Higher epoxy content leads to a higher T_g of the thiol−epoxy/thiol−ene system,[34] which expands the array of polymers that can be co-drawn with this material system. However, excess of epoxy functional groups may yield formation of an insoluble network through thiol−epoxy reaction alone due to the presence of trifunctional TMICN. We found that a composition of the photopolymer network in which 50% of the thiol groups react with epoxy and the other 50% of the thiol groups react with alkene groups offers the highest epoxy content that permits photopatterning following thermal-curing at the time and temperature associated with the typical drawing process. The resulting 2:1:1 (thiol:epoxy:alkene) ratio of the functional groups was then employed in the rest of the experiments in this study.

Unlike other methods that rely on additional post-processing steps to incorporate photoresists into fibers,[27−31] the thiol−epoxy/thiol−ene photopolymer could be drawn together with other materials with similar thermomechanical properties into meters-long integrated fibers in a one-step fabrication process (Figure 3a). In our preform, a macroscopic precursor of the fiber, a single conductor composed of a carbon-loaded polyethylene (CPE) was embedded between the photopolymer and an insulating substrate of cyclic olefin copolymer (COC) (Figure 3b). Although thermal drawing usually maintains the feature aspect ratio, the thickness of the photopolymer layer in the fiber became thinner relative to the original aspect ratio in the preform (Figure 3c). This is likely due to the faster flow of the thermally uncured thiol−epoxy/thiol−ene mixture during thermal drawing in the vertical draw tower. Nevertheless, in the resulting fibers the conductor was fully coated by an over 9 μm photopolymer layer along its entire length. To reduce the flow of the thiol−epoxy/thiol−ene mixture during thermal drawing, the fiber preform can be precured, which increases the mixture viscosity and results in greater photopolymer thicknesses. Consequently, directly following drawing the fibers can be subjected to photolithography.

To photolithographically pattern thermally drawn fibers, they were exposed to the 302 nm light through masks and immersed into acetone over 10 min for development. Similar to photolithography on unstrained free-standing films, patterns with resolution of at least 1 μm were developed directly on the thermally drawn photopolymer demonstrating, for the first time, an in-fiber photolithography with a thermoplastic photoresist (Figure 3d−g). Although here photolithographic patterning was applied to fibers with rectangular cross sections, which are compatible with planar commercially available photomasks, curved or flexible photomasks[28,37] would similarly permit patterning of traditional cylindrical fibers as well as those with more complex cross-sectional structures.

To evaluate whether the photopolymer could provide effective electrical insulation and could also be removed entirely to grant access to the conductor elements within the fibers, line patterns (76 or 330 μm) were developed above the CPE electrodes. The resultant fibers contained electrodes exposed to the surrounding environment at its tip and at the patterned region along its shaft. The electrode impedance was then measured at these two locations (Figure 3h,i). To evaluate the insulating properties of the photopolymer, the fiber tips were encapsulated in epoxy and the fibers were submerged into the phosphate-buffered saline (PBS) to a level below the pattern (schematic 1 in the inset of Figure 3h). The impedance of ∼11.3 MΩ at 1 kHz indicated that the thermally drawn photoresist acts as an insulator following development, which implied that electrical access to conductors isolated with the photopolymer could be deterministically imparted exclusively at the photolithographically exposed locations. When the same fibers were immersed into PBS to a level above the pattern (schematic 2 in the inset of Figure 3h), impedance values of 5.26 ± 0.33 MΩ and 1.98 ± 0.24 MΩ at 1 kHz for 76 and 330 μm patterns, respectively, were observed consistent with prior reports of CPE conductance in similarly sized devices[14,15] (Figure 3h,i). Finally, the epoxy was mechanically removed from the fiber tips exposing the CPE electrodes in that location. The fibers again were immersed in PBS to a level below the pattern revealing tip impedance values of 1.83 ± 0.26 MΩ (for fibers with 76 and 330 μm patterns) consistent with prior reports. Impedances scaling with the exposed electrode areas measured at the tip and at the patterned points indicate complete exposure of the electrodes along the length following in-fiber lithography (Figure 3h,i). Together, these findings demonstrate that the integration of a thermoplastic photoresist at the level of a fiber preform delivers meters-long integrated fibers with customizable patterns along the fiber shaft. These patterns could increase functional utility of fibers by providing access to microdevices integrated along the length, delivering fluids to multiple locations, and sensing a variety of signals at predetermined points. Although coating of photoresists onto fiber surfaces following drawing can deliver

https://dx.doi.org/10.1021/acscentsci.0c01188
ACS Cent. Sci. 2020, 6, 2319−2325

similar benefits (Figure S2), the integration of the drawable photoresists at the macroscale takes advantage of the high-throughput fiber drawing and avoids additional processing steps associated with surface deposition of photoresists onto drawn fibers.

CONCLUSION

Two scalable approaches—photolithography and thermal drawing—were combined for high yield processing of fibers microscopically patternable at arbitrary locations along the length. This was enabled by the development of a thermoplastic photoresist with thermomechanical properties matching those of high-performance plastics and composites. The thermally drawable photoresist consisted of a mixture of trifunctional thiol, bifunctional epoxy, and trifunctional alkene monomers. During thermal curing, partial polymerization of thiol with epoxy groups resulted in a thermoplastic, that could be co-drawn with other elements within a multimaterial fiber. Exposing the resulting fibers to UV light led to photopolymerization between the remaining thiol groups and trifunctional alkene molecules forming an insoluble network. Our approach breaks the longitudinal symmetry characteristic of fibers, while taking advantage of processing of kilometer-scale production of micro- and nanostructured features from macroscopic preforms. By offering access to functional elements within fibers at multiple specified locations, this approach may expand applications of these multifunctional multimaterial structures in flexible, large area devices, advancing textile, sensing, and biomedical industries.

METHODS

Photopolymer Synthesis. For the thiol−epoxy/thiol−ene photopolymer which composed of 2:1:1 ratio of thiol:epoxy:alkene functional groups, first, 2,2-dimethoxy-2-phenylacetophenone (1.0 wt %, DMPA, MilliporeSigma) and butylated hydroxytoluene (0.1 wt %, BHT, MilliporeSigma) were added in melted BADGE (27.6 wt %, MilliporeSigma). DMPA was chosen as a photoinitiator to trigger the photocuring reaction, and BHT was used as a radical inhibitor which prevents overcuring by heat-induced radicals created during long-time thermal curing. Then, TATATO (13.5 wt %, MilliporeSigma), TMICN (56.8 wt %, Alfa Chemistry), and tripropylamine (1.0 wt %, MilliporeSigma) were added to the same vial. Tripropylamine is added to catalyze the thermal curing reaction. The resulting viscous mixture was stirred and degassed over 3 h under vacuum to remove air bubbles. All processes were carried out under the red light.

Patterning on Free-Standing Films. To pattern a free-standing film, the photopolymer mixture was poured to a Teflon mold 500 μm deep and thermally cured at 100 °C in an oven for 4 h. After cooling, the photopolymer was covered with a soda lime/chromium mask (Front Range Photomask) and exposed to UV lamp (UVLM-28, UVP) with a wavelength λ = 302 nm and intensity 16.06−17.47 W/m^2 during 40−50 min. In this paper, the same UV source was used for all photocuring. After photocuring, the samples were immersed into acetone (MilliporeSigma) over 15 min. Among solvents that can dissolve the thermally cured photopolymer, acetone was chosen for pattern development to increase polymer selection for other fiber components which should have resistance to the solvent.

Characterization. For FTIR (FTIR6700, Thermo Fisher), noncured polymer was spin-coated with tetrahydrofuran (MilliporeSigma) on silicon wafer. The thermal curing was performed at 100 °C in an oven (Gravity Convection Ovens, VWR International) for 10 min, and photocuring time was 60 min. The resulting sample thicknesses ranged 2.3−2.5 μm. The reflection mode of the FTIR was used to record the spectra, and a resolution of 4/cm was used to accumulate 128 scans. The results were normalized with peaks of aromatic rings of BADGE in each photopolymer because aromatic ring structure is preserved during all curing steps.

For DSC (Discovery, TA Instruments) measurement, samples were prepared with different thermal curing times at 100 °C in an oven. Three heating and cooling cycles were repeated between −30 and 80 °C for each sample. The heating and cooling rates were 10 and 20 °C/min, respectively. A nitrogen flow of 50 mL/min was used.

Using a UV−vis spectrophotometer (Lambda 1050, PerkinElmer), the transmittance of light with wavelengths between 200 and 800 nm was measured through free-standing films with 500 μm thickness. The samples were thermally cured at 100 °C in an oven for 4 h and photocured for 40 min.

Pattern Imaging. The developed patterns on the photopolymer were coated with a gold film (8 nm) using a sputter coater (SC7640, Quorum Technologies). Images of the samples were taken using scanning electron microscopy (SEM, 6010LA, JEOL).

Thermal Drawing Process. For thermal drawing process, a preform was assembled with a single CPE (Hillas Packaging) electrode located in a channel milled on the COC (8007S-04, TOPAS) substrate and hot-pressed at 125 °C for 1 h to consolidate them. CPE and COC were selected in consideration of their thermomechanical and solvent resistive properties (Table S1). Oxygen plasma treatment was performed on the electrode surface of the preform and the noncured photopolymer was poured on the surface. To reduce flow of the photopolymer during thermal drawing, the preform was precured at 100 °C in an oven at for a period of time within a range of 10−60 min. All precuring times within this range delivered drawable and patternable photopolymer layers within the fibers. Longer precuring time led to thicker photopolymer layers (∼90 μm). After cooling, the preform was thermally drawn at 180 °C using a custom-built draw tower similar to prior work.[14] To prevent overcuring of the photopolymer during the process, we used feed speed of 2.3 mm/min along the vertical furnace. Since the distance between the top and middle points of the furnace is 9 cm, the photopolymer was thermally cured for around 40 min in the draw tower. A range of fiber cross-sectional areas was 0.64−1 mm^2.

Photolithography on Fiber. After thermal drawing, fibers were cut to 5 cm fragments for facile processing. The thermally drawn photoresist was photocured under UV light with covering mask at the desired point to be patterned. While a soda lime/chromium mask was used for general patterning, line patterns for impedance measurement were created using metal (aluminum or nickel−chromium, McMaster-Carr) wires as a mask to prevent damages of photopolymer by attachment to soda lime. For photocuring, 4 min was used with the metal wires, whereas the soda lime/chromium needed longer time of 20−30 min due to an absorption of UV light to soda lime. For pattern development, fibers were immersed in acetone over 10 min.

https://dx.doi.org/10.1021/acscentsci.0c01188
ACS Cent. Sci. 2020, 6, 2319−2325

Fiber Cross-Sectional Imaging. Fibers were embedded in an epoxy (Electron Microscopy Sciences) matrix to fix them vertically and mechanically polished with sandpapers of gradually decreasing grain sizes. The samples were imaged using optical microscope (AmScope).

Impedance Measurement. For impedance measurement, the electrodes at the end of each fiber have to be exposed to connect with external wires. Thermally drawn photopolymer at connection points was also removed by a photolithographic process. The exposed electrodes were connected to Cu wire (McMaster-Carr) with conductive silver paint (SPI Supplies). Then, impedance was measured using a precision LCR meter (HP4284A, Keysight Technologies) with a sinusoidal input (10 mV, 20 Hz−1 MHz) when a closed circuit was designed by fibers and another external wire immersed into PBS (Corning) in a single vial.

■ ASSOCIATED CONTENT

Supporting Information

The Supporting Information is available free of charge at https://pubs.acs.org/doi/10.1021/acscentsci.0c01188.

Thiol−epoxy/thiol−ene reactions; optimization of composition between epoxy and alkene functional groups for thermal drawing; dip coating fibers into the thiol−epoxy/thiol−ene photopolymer; Thermomechanical, solvent resistive, and optical properties of polymers used as fiber components (PDF)

■ AUTHOR INFORMATION

Corresponding Author

Polina Anikeeva − *Department of Materials Science and Engineering, Research Laboratory of Electronics, McGovern Institute for Brain Research, and Department of Brain and Cognitive Sciences, Massachusetts Institute of Technology, Cambridge, Massachusetts 02139, United States;* orcid.org/0000-0001-6495-5197; Email: anikeeva@mit.edu

Authors

Youngbin Lee − *Department of Materials Science and Engineering, Research Laboratory of Electronics, and McGovern Institute for Brain Research, Massachusetts Institute of Technology, Cambridge, Massachusetts 02139, United States*

Andres Canales − *Department of Materials Science and Engineering and Research Laboratory of Electronics, Massachusetts Institute of Technology, Cambridge, Massachusetts 02139, United States*

Gabriel Loke − *Department of Materials Science and Engineering and Research Laboratory of Electronics, Massachusetts Institute of Technology, Cambridge, Massachusetts 02139, United States*

Mehmet Kanik − *Research Laboratory of Electronics and McGovern Institute for Brain Research, Massachusetts Institute of Technology, Cambridge, Massachusetts 02139, United States*

Yoel Fink − *Department of Materials Science and Engineering, Research Laboratory of Electronics, and Institute for Soldier Nanotechnologies, Massachusetts Institute of Technology, Cambridge, Massachusetts 02139, United States*

Complete contact information is available at: https://pubs.acs.org/10.1021/acscentsci.0c01188

Notes

The authors declare no competing financial interest.

■ ACKNOWLEDGMENTS

This project is supported in part by the National Science Foundation (NSF) through the Center for Materials Science and Engineering (DMR-14-19807), the Center for Neurotechnology (EEC-1028725), and by the National Institute of Neurological Disorders and Stroke (5R01-NS086804). Y. L. is a recipient of Kwanjeong Fellowship.

■ REFERENCES

(1) Abouraddy, A. F.; Bayindir, M.; Benoit, G.; Hart, S. D.; Kuriki, K.; Orf, N.; Shapira, O.; Sorin, F.; Temelkuran, B.; Fink, Y. Towards Multimaterial Multifunctional Fibres That See, Hear, Sense and Communicate. *Nat. Mater.* **2007**, *6*, 336−347.

(2) Wang, L.; Fu, X.; He, J.; Shi, X.; Chen, T.; Chen, P.; Wang, B.; Peng, H. Application Challenges in Fiber and Textile Electronics. *Adv. Mater.* **2020**, *32*, 1901971.

(3) Loke, G.; Yan, W.; Khudiyev, T.; Noel, G.; Fink, Y. Recent Progress and Perspectives of Thermally Drawn Multimaterial Fiber Electronics. *Adv. Mater.* **2020**, *32*, 1904911.

(4) Sordo, F.; Janecek, E. R.; Qu, Y.; Michaud, V.; Stellacci, F.; Engmann, J.; Wooster, T. J.; Sorin, F. Microstructured Fibers for the Production of Food. *Adv. Mater.* **2019**, *31*, 1807282.

(5) Gumennik, A.; Stolyarov, A. M.; Schell, B. R.; Hou, C.; Lestoquoy, G.; Sorin, F.; McDaniel, W.; Rose, A.; Joannopoulos, J. D.; Fink, Y. All-in-Fiber Chemical Sensing. *Adv. Mater.* **2012**, *24*, 6005−6009.

(6) Stolyarov, A. M.; Wei, L.; Shapira, O.; Sorin, F.; Chua, S. L.; Joannopoulos, J. D.; Fink, Y. Microfluidic Directional Emission Control of an Azimuthally Polarized Radial Fibre Laser. *Nat. Photonics* **2012**, *6*, 229−233.

(7) Qu, Y.; Nguyen-Dang, T.; Page, A. G.; Yan, W.; Das Gupta, T.; Rotaru, G. M.; Rossi, R. M.; Favrod, V. D.; Bartolomei, N.; Sorin, F. Superelastic Multimaterial Electronic and Photonic Fibers and Devices via Thermal Drawing. *Adv. Mater.* **2018**, *30*, 1707251.

(8) Yu, L.; Parker, S.; Xuan, H.; Zhang, Y.; Jiang, S.; Tousi, M.; Manteghi, M.; Wang, A.; Jia, X. Flexible Multi-Material Fibers for Distributed Pressure and Temperature Sensing. *Adv. Funct. Mater.* **2020**, *30*, 1908915.

(9) Bayindir, M.; Sorin, F.; Abouraddy, A. F.; Viens, J.; Hart, S. D.; Joannopoulos, J. D.; Fink, Y. Metal − Insulator − Semiconductor Optoelectronic Fibres. *Nature* **2004**, *431*, 826.

(10) Sorin, F.; Abouraddy, A. F.; Orf, N.; Shapira, O.; Viens, J.; Arnold, J.; Joannopoulos, J. D.; Fink, Y. Multimaterial Photodetecting Fibers: A Geometric and Structural Study. *Adv. Mater.* **2007**, *19*, 3872−3877.

(11) Chocat, N.; Lestoquoy, G.; Wang, Z.; Rodgers, D. M.; Joannopoulos, J. D.; Fink, Y. Piezoelectric Fibers for Conformal Acoustics. *Adv. Mater.* **2012**, *24*, 5327−5332.

(12) Wei, L.; Hou, C.; Levy, E.; Lestoquoy, G.; Gumennik, A.; Abouraddy, A. F.; Joannopoulos, J. D.; Fink, Y. Optoelectronic Fibers via Selective Amplification of In-Fiber Capillary Instabilities. *Adv. Mater.* **2017**, *29*, 1603033.

(13) Zhang, Q.; Roach, D. J.; Geng, L.; Chen, H.; Qi, H. J.; Fang, D. Highly Stretchable and Conductive Fibers Enabled by Liquid Metal Dip-Coating. *Smart Mater. Struct.* **2018**, *27*, 035019.

(14) Canales, A.; Jia, X.; Froriep, U. P.; Koppes, R. A.; Tringides, C. M.; Selvidge, J.; Lu, C.; Hou, C.; Wei, L.; Fink, Y.; Anikeeva, P. Multifunctional Fibers for Simultaneous Optical, Electrical and Chemical Interrogation of Neural Circuits in Vivo. *Nat. Biotechnol.* **2015**, *33*, 277−284.

(15) Guo, Y.; Jiang, S.; Grena, B. J. B.; Kimbrough, I. F.; Thompson, E. G.; Fink, Y.; Sontheimer, H.; Yoshinobu, T.; Jia, X. Polymer Composite with Carbon Nanofibers Aligned during Thermal Drawing as a Microelectrode for Chronic Neural Interfaces. *ACS Nano* **2017**, *11*, 6574−6585.

(16) Park, S.; Guo, Y.; Jia, X.; Choe, H. K.; Grena, B.; Kang, J.; Park, J.; Lu, C.; Canales, A.; Chen, R.; Yim, Y. S.; Choi, G. B.; Fink, Y.; Anikeeva, P. One-Step Optogenetics with Multifunctional Flexible Polymer Fibers. *Nat. Neurosci.* **2017**, *20*, 612−619.
(17) Canales, A.; Park, S.; Kilias, A.; Anikeeva, P. Multifunctional Fibers as Tools for Neuroscience and Neuroengineering. *Acc. Chem. Res.* **2018**, *51*, 829−838.
(18) Shahriari, D.; Loke, G.; Tafel, I.; Park, S.; Chiang, P. H.; Fink, Y.; Anikeeva, P. Scalable Fabrication of Porous Microchannel Nerve Guidance Scaffolds with Complex Geometries. *Adv. Mater.* **2019**, *31*, 1902021.
(19) Arumugam, S.; Li, Y.; Senthilarasu, S.; Torah, R.; Kanibolotsky, A. L.; Inigo, A. R.; Skabara, P. J.; Beeby, S. P. Fully Spray-Coated Organic Solar Cells on Woven Polyester Cotton Fabrics for Wearable Energy Harvesting Applications. *J. Mater. Chem. A* **2016**, *4*, 5561−5568.
(20) Rein, M.; Favrod, V. D.; Hou, C.; Khudiyev, T.; Stolyarov, A.; Cox, J.; Chung, C. C.; Chhav, C.; Ellis, M.; Joannopoulos, J.; Fink, Y. Diode Fibres for Fabric-Based Optical Communications. *Nature* **2018**, *560*, 214−218.
(21) Torres Alonso, E.; Rodrigues, D. P.; Khetani, M.; Shin, D.-W.; De Sanctis, A.; Joulie, H.; de Schrijver, I.; Baldycheva, A.; Alves, H.; Neves, A. I. S.; Russo, S.; Craciun, M. F. Graphene Electronic Fibres with Touch-Sensing and Light-Emitting Functionalities for Smart Textiles. *npj Flex. Electron.* **2018**, *2*, 25.
(22) Zhang, T.; Wang, Z.; Srinivasan, B.; Wang, Z.; Zhang, J.; Li, K.; Boussard-Pledel, C.; Troles, J.; Bureau, B.; Wei, L. Ultraflexible Glassy Semiconductor Fibers for Thermal Sensing and Positioning. *ACS Appl. Mater. Interfaces* **2019**, *11*, 2441−2447.
(23) Zhang, J.; Uzun, S.; Seyedin, S.; Lynch, P. A.; Akuzum, B.; Wang, Z.; Qin, S.; Alhabeb, M.; Shuck, C. E.; Lei, W.; Kumbur, E. C.; Yang, W.; Wang, X.; Dion, G.; Razal, J. M.; Gogotsi, Y. Additive-Free MXene Liquid Crystals and Fibers. *ACS Cent. Sci.* **2020**, *6*, 254−265.
(24) Naguib, M. Multifunctional Pure MXene Fiber from Liquid Crystals of Only Water and MXene. *ACS Cent. Sci.* **2020**, *6*, 344−346.
(25) Nayak, K. P.; Hakuta, K. Photonic Crystal Formation on Tapered Optical Nanofibers Using Femtosecond Laser Ablation Technique. *Opt. Express* **2013**, *21*, 2480−2490.
(26) Boyd, K.; Rees, S.; Simakov, N.; Daniel, J. M. O.; Swain, R.; Hemming, A.; Clarkson, W. A.; Haub, J. High Precision 9.6 Mm CO2 Laser End-Face Processing of Optical Fibres. *Opt. Express* **2015**, *23*, 15065−15071.
(27) Sasaki, M.; Ando, T.; Nogawa, S.; Hane, K. Direct Photolithography on Optical Fiber End. *Jpn. J. Appl. Phys.* **2002**, *41*, 4350−4355.
(28) Lu, Y.; Zhang, Y.; Lu, J.; Mimura, A.; Matsumoto, S.; Itoh, T. Three-Dimensional Photolithography Technology for a Fiber Substrate Using a Microfabricated Exposure Module. *J. Micromech. Microeng.* **2010**, *20*, 125013.
(29) Kostovski, G.; Chinnasamy, U.; Jayawardhana, S.; Stoddart, P. R.; Mitchell, A. Sub-15nm Optical Fiber Nanoimprint Lithography: A Parallel, Self-Aligned and Portable Approach. *Adv. Mater.* **2011**, *23*, 531−535.
(30) Kostovski, G.; Stoddart, P. R.; Mitchell, A. The Optical Fiber Tip: An Inherently Light-Coupled Microscopic Platform for Micro- and Nanotechnologies. *Adv. Mater.* **2014**, *26*, 3798−3820.
(31) Babkin, O. E.; Babkina, L. A.; Aikasheva, O. S.; Il'ina, V. V. Photopolymeric Coatings for Fiber-Optic Cables. *Fibre Chem.* **2019**, *50*, 499−503.
(32) Crivello, J. V.; Reichmanis, E. Photopolymer Materials and Processes for Advanced Technologies. *Chem. Mater.* **2014**, *26*, 533−548.
(33) Sahin, M.; Ayalur-Karunakaran, S.; Manhart, J.; Wolfahrt, M.; Kern, W.; Schlögl, S. Thiol-Ene versus Binary Thiol−Acrylate Chemistry: Material Properties and Network Characteristics of Photopolymers. *Adv. Eng. Mater.* **2017**, *19*, 1600620.
(34) Sangermano, M.; Cerrone, M.; Colucci, G.; Roppolo, I.; Ortiz, R. A. Preparation and Fcharacterization of Hybrid Thiol-Ene/Epoxy UV-Thermal Dual-Cured Systems. *Polym. Int.* **2010**, *59*, 1046−1051.
(35) Ware, T.; Simon, D.; Hearon, K.; Kang, T. H.; Maitland, D. J.; Voit, W. Thiol-Click Chemistries for Responsive Neural Interfaces A. *Macromol. Biosci.* **2013**, *13*, 1640−1647.
(36) Higashihara, T.; Ueda, M. Recent Progress in High Refractive Index Polymers. *Macromolecules* **2015**, *48*, 1915−1929.
(37) Kim, J. G.; Takama, N.; Kim, B. J.; Fujita, H. Optical-Softlithographic Technology for Patterning on Curved Surfaces. *J. Micromech. Microeng.* **2009**, *19*, 055017.

https://dx.doi.org/10.1021/acscentsci.0c01188
ACS Cent. Sci. 2020, 6, 2319−2325